CrystEngComm

Accepted Manuscript

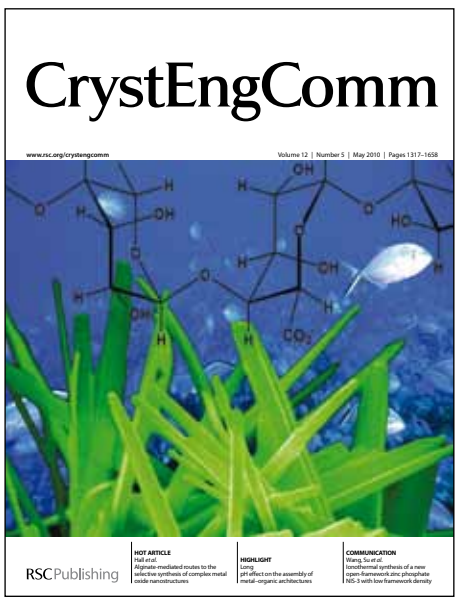

Journal Name

RSCPublishing

ARTICLE

Halogen bonding directed Supramolecular Assembly in Bromo-substituted Trezimides and Tennimides

Cite this: DOI: 10.1039/x0xx00000x

Pavle Mocilac and John F. Gallagher*[a]

Received 00th January 2012,
Accepted 00th January 2012

DOI: 10.1039/x0xx00000x

www.rsc.org/

Reaction of isophthaloyl dichloride (**I**) with 2-amino-5-bromopyridine (**BrO**) and 2-amino-5-bromopyrimidine (**26BrO**) produces the trimeric (**trezimide**) and tetrameric (**tennimide**) imide–based macrocycles (**BrIO**)$_3$, (**BrIO**)$_4$ and (**26BrIO**)$_3$, (**26BrIO**)$_4$, respectively, in one-step and in modest yields. Macrocyclisation (forming 18–/24–membered rings) is facilitated by the imide *hinge* [O=C–N(*R*)–C=O] (*R=ortho-N*-substituted-pyridine/pyrimidine) though competing reactions also lead to considerable oligomer/polymer formation. The macrocycles (having 3 or 4 Br atoms) lack classical strong hydrogen bonding donors (i.e. N–H, O–H), but contain numerous acceptors (i.e. $N_{aromatic}$, C=O, arene) participating in halogen and weaker hydrogen bonding. Five crystal structures are analysed with the macrocycles typically aggregating through short C–Br…O=$C_{carbonyl}$ and/or C–Br…$N_{aromatic}$ halogen bonds ($N_c \leq 0.90$) and often associated with longer C–Br…H/π(arene) contacts. Of note, (**BrIO**)$_3$ exhibits three types of Br…O=C/π(arene) halogen bonds, and with Br...H and C–H…O contacts. The C–Br…N/O halogen bonds in promoting overall aggregation typically link macrocycles into 1–D halogen bonded chains.

Introduction

Benzoyl chlorides readily react with 2-aminopyridine (2-AP) in dichloromethane (CH_2Cl_2) at ambient temperatures in the presence of triethylamine (Et_3N) to yield *N*-benzoyl-*N*-pyridin-2-yl-benzamides (2:1 imides) and often in preference to the expected (1:1) benzamide products.[1-2] This dibenzoylation reaction is well known, having first been reported by Marckwald in 1894.[1] Subsequent publications have expanded on this condensation reaction during the 20th/21st centuries by examining the reaction mechanism, kinetics and structures.[2] However, given the plethora of benzamides reported as scaffolds in drugs and materials, the *open-chain* imides have not been exploited in any particular synthetic route or application. As such, the Pubchem database[3] reveals some 150 substructures based on the *N*-benzoyl-*N*-pyridin-2-yl-benzamide (imide) system, though with many derivatives reported as members of drug design compound libraries,[3] while detailed analysis reveals > 300 *N*,*N*-dibenzoylanilines including the 6-p-phenyl-dibenzo[*c*,*e*]azepine-5,7-diones.[4]

Imides (when incorporated into aromatic rings) are ubiquitous in materials science, with polyimides (based on e.g. naphthalene-tetracarboxylic diimides developed during the 1950's) playing important roles in various technological applications.[5] The research focus on imides in supramolecular (as well as in macrocyclic chemistry) has largely grown from their potential usage in a wide variety of applications based on their spectroscopic and electronic properties.[6-8] Macrocyclic imides have been developed and typically derive from pyromellitic[6] and perylene bisimides;[7] together with naphthalene-diimides, these almost exclusively incorporate rigid aromatic imide components.[6-8] Such planar diimides contrast with the relatively unexplored *open-chain* and more flexible macrocyclic tetrameric imides as first reported on by Evans and Gale in 2004.[9,10]

Interest has also surged recently in what have been regarded hitherto as non-standard intermolecular interactions as exemplified by hydrogen C–H…X (X = I/Br/Cl/F) and halogen C–X…O=C/$N_{alkyl/aromatic}$ bonding.[11,12] The appeal, especially of the C–(Br/I)…O=C/N halogen bonding, stems for example from the ability of perfluorinated(Br/I) alkyl and aromatic systems to induce a positive σ-hole on the neighbouring bromine/iodine atoms (as analysed from structural data and computational methods[11,12]). Research is on-going to exploit and fully understand halogen bonding (and σ-holes) in crystal engineering, material science and biological research.[10-12]

Halogenated macrocycles[10] play key roles in the development of new materials and derivatives by utilising their rich reaction chemistry, especially where Br, I atoms are present.[11-12] Given the immense interest in halogen bonding, the present study was undertaken to try to understand the critical role of halogen bonds in macrocycles lacking strong hydrogen bond donors but with an excess of acceptors. Herein, the reaction of isophthaloyl dichloride (**I**) with 2-amino-5-bromopyridine (**BrO**) and 2-amino-5-bromopyrimidine (**26BrO**) produces trimeric (**trezimide**) and tetrameric (**tennimide**) imide-based macrocycles in one-step and in

modest yields as **(BrIO)$_3$**, **(BrIO)$_4$** (from 2-amino-5-bromopyridine) and **(26BrIO)$_3$**, **(26BrIO)$_4$** (using 2-amino-5-bromopyrimidine), respectively, (Scheme 1).[13] Formation of the imide *hinge* as –A[C(=O)–N(*R*)–C(=O)]–$_n$ (A = aromatic linker, *R* = (hetero)aromatic ring, *n* = 3/4) and subsequent macrocyclisation provides an entry point into two relatively unexplored classes of imide-based macrocycle.[9,13] Recently, the parent trimeric (**trezimide**) and tetrameric (**tennimide**) macrocycles **(IO)$_{3/4}$** and **(26IO)$_{3/4}$**,[13a] and **(EsIO)$_{3/4}$** macrocyclic esters[13b] have been reported (where H[13a] or CO_2Me[13b], respectively, replace the Br atoms in Scheme 1).

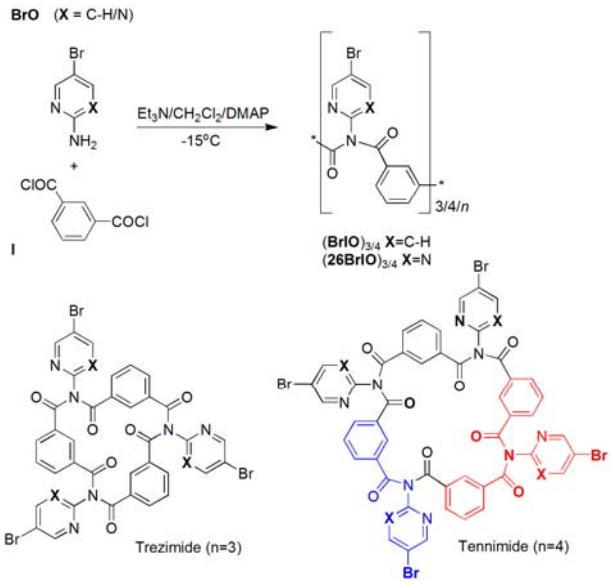

Scheme 1. Synthesis of **(BrIO)$_{3/4}$** and **(26BrIO)$_{3/4}$** (top) and schematics of the macrocyclic trezimide and tennimide (bottom). In the tennimide, benzamide (**blue**) and imide (**red**) components are highlighted.

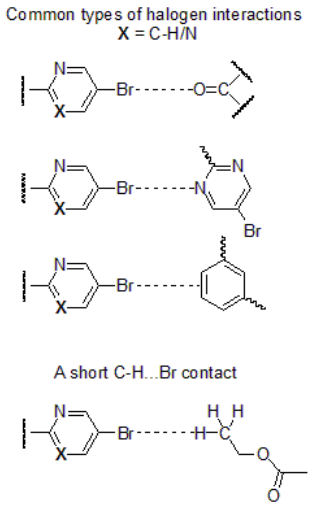

Scheme 2. Main types of Br...O=C/N/π(arene) halogen bonding in **(BrIO)$_{3/4}$** and **(26BrIO)$_{3/4}$**; the short Br...H-C contact in **(BrIO)$_3$** (ethyl acetate solvate)

The reactions and structural analyses of the four tri- and tetra-brominated **trezimide**/**tennimides** is discussed together with addressing short halogen (involving Br) and hydrogen bonding interactions in five crystal structures.[13-15] The directional properties of the short C–Br…O=$C_{carbonyl}$ and/or C–Br…$N_{aromatic}$ halogen bonds (with $N_c \leq 0.90$) is assessed especially in 1–D chain formation. Short C–Br...O=C halogen bonding interactions are present in **(26BrIO)$_3$** (with $N_c \leq 0.90$), whereas C–Br…$N_{pyrimidyl}$ intermolecular interactions dominate in **(26BrIO)$_4$** (Scheme 2, motifs). Analysis of short C–Br...O=C/N interactions in the absence of neighbouring C–F moieties (for the five structures) is important in order to assess the role and effect of the positive σ-hole on the Br atoms (with only neighbouring aromatic C–H groups),[11m-n,12] and the resulting halogen bonding interactions.

Experimental section

General synthesis and chromatography

The synthetic procedures for both **(BrIO)$_{3/4}$** and **(26BrIO)$_{3/4}$** reactions are similar, though with some minor technical differences and mainly due to the TLC mobile phase composition. Full details are available in the Supporting Information (SI). Typically the reaction medium was prepared by dissolving DMAP (10 mg, 0.08 mmol) and triethylamine (4 ml, 29.8 mmol) in 80 (60) ml of anhydrous CH_2Cl_2. The 2-amino-5-bromopyridine (1.6964 g, 9.8 mmol) was suspended in 20 ml of anhydrous CH_2Cl_2. For the **(26BrIO)$_{3/4}$** synthesis, 2-amino-5-bromopyrimidine was used (1.7053 g, 9.8 mmol) and suspended in 40 ml of anhydrous CH_2Cl_2. Isophthaloyl dichloride (1.98 g, 9.8 mmol) was dissolved with stirring in 80 ml of reaction media in a 250 ml round bottom flask under N_2 and cooled on an ice bath to –15°C. The 2-amino-5-bromopyridine/pyrimidine suspension was quickly and quantitatively added to the cooled flask containing isophthaloyl dichloride. The reaction mixture was stirred overnight, then diluted with technical grade CH_2Cl_2 to 200 ml, filtered over a funnel with a sintered glass frit to remove a polymeric product, washed with aqueous solutions of NH_4Cl (pH ≈ 5, 3 × 200 ml), dried over $MgSO_4$ and filtered. The solvent was removed to afford a dark red resin and immediately purified by column chromatography on silica gel (Davisil, 70 μm, 82 g, column dimension: *l* = 25 cm, *d* = 3 cm) eluting with a mobile phase of $CHCl_3$/ethyl acetate (4:1) to yield clean, pure macrocyclic products.

Spectroscopy

The spectroscopic and characterisation data including VT ^{1}H-NMR, (20°C→80°C; 120°C), high temperature (80°C; 120°C; 140°C for **(26BrIO)$_4$**) experiments of ^{1}H-NMR, COSY, NOESY, ^{13}C-NMR, DEPT, DEPT-Q, HSQC and HMBC, with IR spectra for **(BrIO)$_3$**, **(BrIO)$_4$**, **(26BrIO)$_3$**, **(26BrIO)$_4$** are provided in the Supporting Information, Sections 2–4. All ^{1}H and ^{13}C NMR experiments were run in DMSO-d_6 using a 600 NMR Spectrometer (14.1 T); the proton and carbon assignments correspond with their labels in the Supporting Information. The FTIR experiments were run using the ATR

technique and mass spectra recorded on a Q-Tof micro quadrupole MS with electron spray ionisation. The four macrocycles correspond with their molecular weights and isotope substitution patterns (Br_3/Br_4) from cluster analysis with evidence for molecular ions (+ H^+, Na^+ or K^+) in all samples.

Analysis by Single crystal diffraction

Selected structural information is provided in Tables 1–2 with full experimental and geometric details as Tables 1–5 in Section 5 of the Supporting Information (SI). The CCDC codes are **930689** to **930693**. Structure solution, refinements[16] and molecular diagrams[17] are as detailed previously.[13,14] Crystal structure analyses were performed on the Cambridge Structural Database (CSD) version 5.34+3 updates.[15]

Synthetic and spectroscopic data

(**BrIO**)$_3$: White crystalline solid, 212 mg (7%); NMR, 80°C, DMSO-d_6; ^{1}H-NMR δ 7.21 (1H, s, H26), 7.76 (1H, t, ^3J = 8, H15), 8.01 (2H, d, ^3J = 8, H14), 8.04 (1H, d, ^3J = 8, H25), 8.16 (1H, s, H23), 8.21 (1H, s, H12); ^{13}C-NMR, δ 118.01, 122.74, 127.66, 130.40, 133.65, 134.52, 141.33, 149.10, 150.70, 171.12; ATR-FTIR, 3064 (w), 2924 (w), 2853 (w), 1712 (s), 1686 (s), 1674 (s), 1600 (m), 1573 (m), 1456 (s), 1368 (m), 1343 (m), 1292 (s), 1274 (s), 1245 (s), 1212 (s); HR-MS (ESI) *m/z* = 906.91471 for $[MH]^+$ (calcd. for $C_{39}H_{21}Br_3N_6O_6$, 906.92).
(**BrIO**)$_4$: White crystalline solid, 177 mg (6%); NMR, 80°C, DMSO-d_6; ^{1}H-NMR, δ 7.10 (1H, s, H26), 7.59 (1H, s, H25), 7.73 (2H, s, H23/H15), 7.82 (1H, s, H12), 7.98 (2H s, H14); ^{13}C-NMR, δ 118.58, 123.43, 127.40, 130.51, 133.50, 134.19, 140.95, 149.40, 151.12, 171.01; ATR-FTIR, 3069 (w), 2956 (w), 2923 (w), 2853 (w), 1709 (s), 1680 (s), 1601 (w), 1571 (m), 1461 (m), 1369 (m), 1311 (s), 1284 (s), 1213 (s); HR-MS (ESI) *m/z* = 1208.88347 for $[MH]^+$ (calcd. for $C_{52}H_{29}Br_4N_8O_8$, 1218.88).
(**26BrIO**)$_3$: White crystalline solid, 164 mg (6%); NMR, 80°C, DMSO-d_6; ^{1}H-NMR δ 7.81 (1H, t, ^3J = 8), 8.10 (2H, dd, ^3J = 8, ^4J = 2), 8.19 (1H, d, ^3J = 1), 8.68 (2H, s); ^{13}C-NMR, δ 116.92, 127.62, 130.82, 133.85, 134.29, 157.00, 159.34, 170.55; ATR-FTIR, 3058 (w), 3008 (w), 2923 (w), 1733 (s), 1702 (s), 1666 (s), 1603 (w), 1547 (w), 1481 (w), 1411 (s), 1372 (m), 1338 (s), 1287 (s), 1215 (s); HR-MS (ESI) *m/z* = 909.90041 for $[MH]^+$ (calcd. for $C_{36}H_{19}Br_3N_9O_6$, 909.9).
(**26BrIO**)$_4$: White crystalline solid, 110 mg (4%); NMR, 140°C, DMSO-d_6; δ 7.84 (1H, t, ^3J = 2), 7.90 (1H, t, ^3J = 8), 7.94 (2H, s), 8.10 (2H, dd, ^3J = 8, ^4J = 2); ^{13}C-NMR, δ 117.26, 126.55, 130.98, 134.00, 134.05, 157.32, 158.92, 170.55; ATR-FTIR, 3057 (w), 3006 (w), 2961 (w), 2923 (w), 2853(w), 2727 (w), 1721 (s), 1682 (s), 1603 (w), 1585 (w), 1546 (s), 1410 (s), 1371 (w), 1310 (s), 1291 (s), 1264 (m), 1237 (m), 1216 (s); HR-MS (ESI) *m/z* = 1212.86488 for $[MH]^+$ (calcd. for $C_{48}H_{24}Br_4N_{12}O_8$, 1212.87).

Oligomer and Polymer (BrIO/26BrIO)$_n$ formation[18]

Macrocycle (**trezimide**/**tennimide**) synthesis occurs along with the formation of short-chain oligomeric imides and polymers (polyimides).[5] These presumably consist of medium and longer-sized spiral chains with free terminal carboxylic acid and/or amide groups, the former generated through partial deactivation of terminal acyl chlorides with adventitious moisture, (Scheme 3).

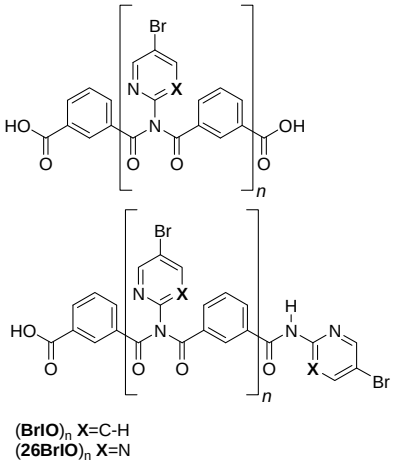

(**BrIO**)$_n$ **X**=C-H
(**26BrIO**)$_n$ **X**=N

Scheme 3. Two of the proposed oligomer and polymer structural types.

The standard strategy in preventing polymer formation is use of the high dilution technique, but for this reaction the approach is not a choice. Instead, cooling the reaction mixture (to −15°C) and slowing the reaction assists in macrocycle formation. Polymer formation usually becomes noticeable with the reaction mixture clouding over (after 30 minutes from the reaction onset). On warming to ambient temperature the polymer becomes more visible and deposits as a gel-like material on the reaction flask.

During filtration using a sintered funnel, the polymeric material (as a gel) shrinks and thickens into a paste as it loses solvent (usually CH_2Cl_2). On drying, it hardens and solidifies into a hard, brittle solid that is insoluble in water and most organic solvents. Once dry and hard, it also proves reluctant to re-absorb solvents and the solidification process appears to be irreversible. As it is relatively brittle, it can be easily obtained in a powdered form with a mortar and pestle and on contact with concentrated and warm acids (e.g. H_2SO_4), the polymeric imide material undergoes rapid degradation.

Results and Discussion

Our research has recently focused on structural systematic studies of $n \times m$ isomer grids of halobenzamides.[14] For benzamides, when condensing acyl chlorides with *ortho*-aminopyridines/pyrimidines, the additional *open-chain* (2:1) imides[1,2] (e.g. **Fxod**,[2h,i] **Mxod**; **F** = fluorine, **M** = methyl, **x** = *para*-/*meta*-/*ortho*-; as **red** component in Scheme 1; SI, Section 5.6) are usually isolated as the major product. Analysis of the CSD[15] for imide analogues[2h,i] revealed the imide–based macrocyclic tetramers (IYURAV/IYUQUO)[9] synthesised from condensation of (**I**) with tetra-/pentafluoroanilines by using the

electron-withdrawing ability of 4–5 F atoms to effect complete $-NH_2$ deprotonation).[9,15] Structural overlay of **Fmod** with ⅜ of the IYURAV/IYUQUO tetramer scaffold non-H atoms[9,15] demonstrates a reasonable overlap. Given the structural similarity, synthesis of *N*-heteroaromatic ring tetramer analogues[9,15] was postulated, then undertaken using 2-aminopyri(mi)dine (Scheme 4; **Fmod**[2h] with a **tennimide**).[13] The *ortho*-$N_{pyri(mi)dine}$ atom in labilising the N–H group and smaller steric size of the flanking *ortho*-N/C–H[13] vs. C–F

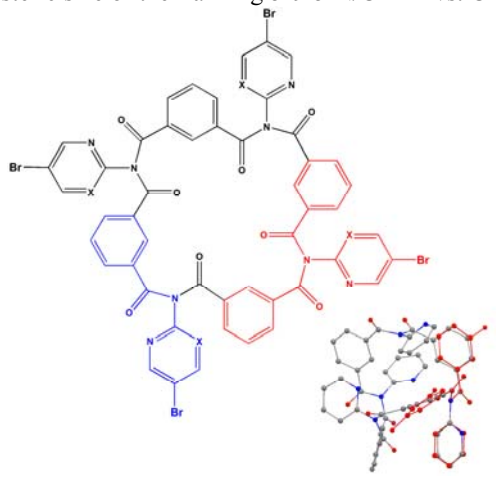

Scheme 4. **Tennimide** core and structural overlay with **Fmod**[2h] (bottom right).

groups are key factors in macrocycle formation.[9] From this work, a major aim is the development of functional macrocycles incorporating heteroaromatic groups for new organic and materials chemistry; this approach has proven feasible using conditions similar to those of Evans & Gale.[9]

Herein, brominated–**trezimides**/**tennimides** macrocycles are discussed and these will be a major focus in future synthetic chemistry (coupling/derivatisation reactions)[19] and in materials science (halogen bonding studies and applications).[11,12]

Synthesis and characterisation

Two synthetic routes (using low/high dilution) to generate macrocycles using *ortho*-aminopyridines/pyrimidines have thus far been explored though the former is preferred, with reactions yielding trimers (**trezimides**) and tetramers (**tennimides**).[13] Therefore, isophthaloyl dichloride is reacted with the 2-amino-5-bromopyri(mi)dines in dry CH_2Cl_2 solvent at −15°C using standard protocols, in the presence of a 3−fold excess of Et_3N and a catalytic quantity of dimethylaminopyridine (DMAP). After standard work-up and purification by column chromatography (silica), two products are isolated and characterised as a **trezimide** and **tennimide** in final isolated yields of 7%, 6% for **(BrIO)$_3$**, **(BrIO)$_4$** and 6%, 4% for **(26BrIO)$_3$**, **(26BrIO)$_4$**. These **(BrIO)$_3$**, **(BrIO)$_4$** and **(26BrIO)$_3$**, **(26BrIO)$_4$** macrocycles have been characterised by spectroscopic and single crystal X-ray diffraction techniques (as five crystal structures as presented in Figures 1–5).

Table 1. Crystal structure details for **(BrIO)$_3$**, **(BrIO)$_4$**, **(26BrIO)$_3$**,[†‡] and **(26BrIO)$_4$**.

Compound	**(BrIO)$_3$**	**(BrIO)$_4$**	**(26BrIO)$_3$**[†]	**(26BrIO)$_3$**[‡]	**(26BrIO)$_4$**
Crystal data, data collection and refinement details[1]					
Chemical formula[2]	$2(C_{39}H_{21}Br_3N_6O_6)$ $\cdot C_4H_8O_2$	$C_{52}H_{28}Br_4N_8O_8$ $\cdot 0.8(CHCl_3)$	$C_{36}H_{18}Br_3N_9O_6$ $\cdot 2(CHCl_3)$	$C_{36}H_{18}Br_3N_9O_6$ $\cdot 2(CH_2Cl_2)$	$2(C_{48}H_{24}Br_4N_{12}O_8)$ $\cdot 3.8(CHCl_3)\cdot H_2O$
*M*r	1906.74	1307.96	1151.06	1082.18	2904.40
Crystal system, space group	Monoclinic, $P2_1/n$	Orthorhombic, *Pccn*	Triclinic, $P\bar{1}$	Triclinic, $P\bar{1}$	Monoclinic, $P2_1/n$
a, *b*, *c* (Å)	10.9440(3) 65.6499(13) 11.2294(3)	14.0441(4) 19.1432(3) 19.1482(4)	12.8150(6) 13.6159(5) 25.7452(11)	12.2390(5) 13.6149(5) 13.6447(5)	10.5779(3) 13.2805(3) 40.7855(13)
α, β, γ (°)	90, 110.447(3), 90	90, 90, 90	84.442(3), 87.666(4), 80.070(4)	100.749(3), 99.990(3), 95.463(3)	90, 95.936(2), 90
V (Å^3), *Z*	7559.7(3), 4	5148.0(2), 4	4402.8(3), 4	2180.69(14), 2	5698.8(3), 2
μ(mm^{-1})	3.26	5.50	3.17	3.08	3.16
Crystal size (mm)	0.52×0.29×0.08	0.35×0.13×0.09	0.34×0.17×0.04	0.49×0.38×0.15	0.39×0.35×0.22
T_{min}, T_{max}	0.282, 0.780	0.249, 0.638	0.412, 0.884	0.314, 0.656	0.372, 0.544
Measured, Independent, Observed [$I>2\sigma(I)$], R_{int}	32690, 15826, 10079, 0.051	30530, 4178, 3574, 0.039	38013, 18957, 8469, 0.058	16290, 9391, 5817, 0.024	41540, 12192, 7949, 0.046
$R[F^2>2\sigma(F^2)]$, $wR(F^2)$, *S(GoF)*	0.075, 0.159, 1.10	0.044, 0.122, 1.04	0.079, 0.193, 1.01	0.067, 0.187, 1.01	0.076, 0.205, 1.03
Reflections, Parameters, Restraints	15826, 1047, 0	4178, 457, 170	18957, 1153, 30	9391, 568, 47	12192, 754, 39
$\Delta\rho_{max}$, $\Delta\rho_{min}$ (e Å^{-3})	0.69, –0.83	0.97, –0.66	1.26, –1.19	1.45, –1.29	1.16, –1.22

Computer programs: *CrysAlis PRO*, Agilent Technologies, Version 1.171.34.49 (release 20-01-2011 CrysAlis171 .NET) (compiled Jan 20 2011, 15:58:25), *SHELXS97* (Sheldrick, 2008), *SHELXL97* (Sheldrick, 2008) and SORTX (McArdle, 1995), *PLATON* (Spek, 2009), *SHELXL97*. [†] $CHCl_3$ solvate and [‡] CH_2Cl_2 solvate of **(26BrIO)$_3$**.[1] Experiments were undertaken at 294 K with a Xcalibur, Sapphire3, Gemini Ultra diffractometer using Mo *K*α radiation (Cu *K*α for **(BrIO)$_4$**) and an analytical absorption correction, (ABSFAC, Clark and Reid, 1998). Data were collected to at least 25° (on θ). H atom parameters were constrained in refinement. The primary solvent used for crystal growth is incorporated into the lattice in each structure.[2]

Table 2. Summary of the C–Br…O=C/$N_{pyrimidine}$/$C_{\pi(arene)}$ halogen bonding interactions.

Trezimide/**Tennimide** Br…O/N/C_π (Å) [$\boldsymbol{N_c}$][11,12]	Br…O=C/N/C_π(arene) (°)	C–Br…O/N/C_π(arene) (°)
(BrIO)$_3$[#]		
Br3B…O6B[1] 3.167(4) [**0.94**]	Br3B…O6B[1]=C6B[1] 135.8(4)	C34B–Br3B…O6B[1] 160.5(2)
Br3A…C15[2] 3.424(6) [**0.97**]	-	C34A–Br3A…C15[2] 169.5(2)
(26BrIO)$_3$[†]		
Br1A…O4A[3] 3.036(4) [**0.90**]	Br1A…O4A[3]=C4A[3] 97.0(4)	C14A–Br1A…O4A[3] 150.9(2)
Br1A…C4A[3] 3.407(6) [**0.96**]	Br1A…C4A[3]=O4A[3] 62.2(4)	C14A–Br1A…C4A[3] 154.4(3)
Br1B…O4B[4] 2.955(4) [**0.88**]	Br1B…O4B[4]=C4B[4] 113.2(4)	C14B–Br1B…O4B[4] 171.9(3)
Br2A…C34[5] 3.366(6) [**0.95**][*]		C24A–Br2A…C34[5] 147.0(3)
Br2B…C64[6] 3.404(7) [**0.96**][*]		C24B–Br2A…C64[6] 147.2(2)
(26BrIO)$_3$ [‡]		
Br14…O4[7] 2.982(3) [**0.89**]	Br14…O4[7]=C4[7] 111.7(3)	C14–Br14…O4[7] 149.39(7)
Br24…C35[8] 3.362(6) [**0.95**][*]		C24A–Br24…C35[8] 162.8(2)
(26BrIO)$_4$ (as Br...$N_{pyrimidine}$)		
Br24…N16A[4] 3.028(5) [**0.89**]	Br24…N16A[4]…C13A[4] 139.0(2)	C24A–Br24…N16A[4] 165.5(2)

[†] $CHCl_3$ and [‡] CH_2Cl_2 are (**26BrIO**)$_3$ solvates; [#] = Br1A...H4S3 hydrogen bond contact, Br...H = 2.69 Å, Br...H–C, C–Br...H angles of 172° and 169°; * = C–Br…π(arene) interaction; Symmetry operations: [1] = –1/2+x, 1/2–y, –1/2+z; [2] = 2–x, –y, –z; **(BrIO)$_3$**. [3] = x, y–1, z; [4] = x, 1+y, z; [5] = –x, 1–y, –z; [6] = 1–x, 1–y, 1–z; **(26BrIO)$_3$**. [7] = x, y, 1–z and [8] = –x, 1–y, 2–z.

Solubility problems hinder the **(26BrIO)$_{3/4/n}$** reaction with the overall effect of limiting higher yields (see below). In addition to the **trezimides** and **tennimides**, the formation of high molecular weight oligomers and polymeric materials (Scheme 1, *n*; Scheme 3) is noted with these products isolated and separated during the standard organic product work-up.

As 2-amino-5-bromopyrimidine is quite insoluble in dry CH_2Cl_2, (even upon warming) it was added to the reaction mixture as a suspension. In comparison with the related F/Cl macrocycles, the solubility of both **(BrIO)$_3$**/**(BrIO)$_4$** is broadly similar (soluble in CH_2Cl_2, $CHCl_3$, alcohols, acetone, THF, ethyl acetate, yet poorly soluble in diethyl ether and *n*-hexane, insoluble in water) but lower than the F/Cl analogues and especially so for **(BrIO)$_4$**. This is not surprising as the starting material (2-amino-5-bromopyridine) is much less soluble in CH_2Cl_2 than for the F/Cl analogues. The **(26BrIO)$_3$**/**(26BrIO)$_4$** macrocycles proved to be relatively insoluble; however, with **(26BrIO)$_3$** more soluble than **(26BrIO)$_4$** (that proved very insoluble in most organic solvents and even in warm DMSO). The NMR and IR results (^{1}H- and ^{13}C-NMR data at 80°C as presented in the Supporting Information) have confirmed the identity of all four macrocycles. Given its poor solubility, NMR characterisation of **(26BrIO)$_4$** was performed in DMSO-d_6 at 140°C using a variable temperature (VT) run, but this relatively high temperature causes partial macrocycle disintegration. Therefore, ^{1}H-NMR VT analysis was undertaken from higher to lower temperature to limit the rate of decomposition. The infra-red data display the expected C=O bands and show additional peaks around 3000 cm^{-1} suggesting that the bulk **(BrIO)$_4$** is a solvate, but not **(BrIO)$_3$**. Overall, product yields are modest and the isolated (fully purified) yields are influenced both by solubility and competing reactions that give rise to longer chain oligomers and polymers (Scheme 3).[18]

Crystal Structures: Imide hinge, isophthaloyl group and halogen bonding analysis

The structures of the four macrocycles **(BrIO)$_3$**, **(BrIO)$_4$**, **(26BrIO)$_3$**, (ex–CH_2Cl_2 and $CHCl_3$ solvates) and **(26BrIO)$_4$** were determined using standard protocols [Mo radiation, with Cu–Kα used for **(BrIO)$_4$**].[13,14] Crystals were grown slowly from a range of solvents at room temperature with all five crystal structures containing solvent molecules of known composition (though often present as partial occupancy and disordered molecules in the lattice voids). The crystal structure determinations with selected geometric data are summarised in Tables 1–2, depicted in Figures 1–5 and with full structural details (interactions with symmetry codes) in the Supporting Information (Tables 1–5, SI).

(BrIO)$_3$ crystallises with two macrocycles (A, B) and a solvent molecule of ethyl acetate in the asymmetric unit (Figure 1a). Both A and B macrocycles are asymmetric in shape with bowl-shaped molecular niches (Figure 1) and they differ significantly from one another (Table 2). The ethyl acetate partially resides in the molecular niche of macrocycle A and participating in two C–H…O=C interactions involving O1S and O4A (Figure 1a,c,d) (geometric details/symmetry codes in SI). Macrocycle A nestles into the niche of macrocycle B as defined by atoms O2B/O4B/O5B with the C3A=O3A carbonyl group and C24–H24 moieties protruding into the macrocyclic niche at contact distances (Figure 1b); this type of inclusion (as well as complete enclathration) is well-known.[10,15,20]

The three molecules do not exhibit disorder apart from vibrational motion/disorder associated with the Br2(A/C) and Br2(B/D) atoms and the pyridyl rings to which they are attached. These bromine sites are located in the lattice such that they are devoid of significant intermolecular contacts.

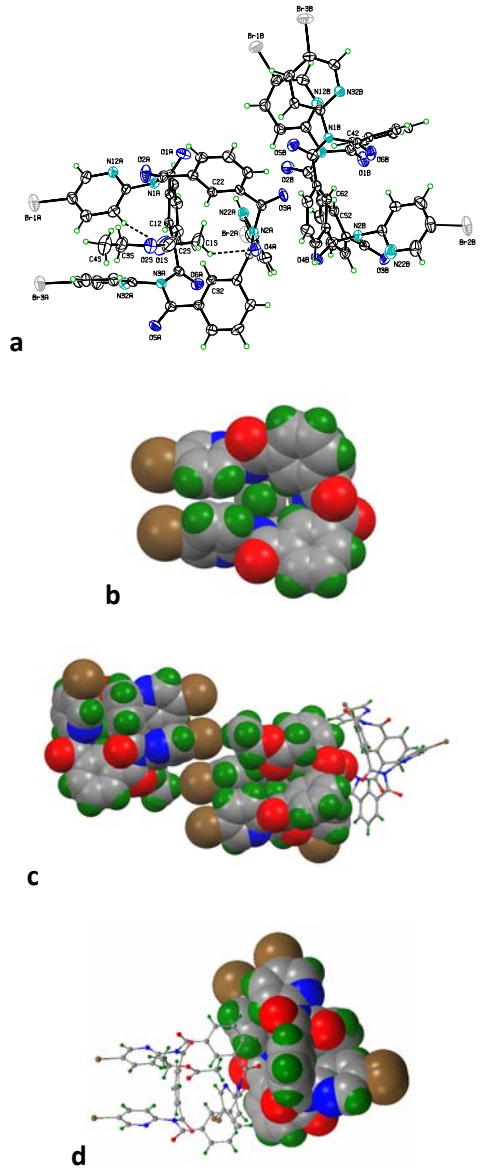

Figure 1. Views of (**BrIO**)$_3$ as (a) an ORTEP of the asymmetric unit (without disorder) with displacement ellipsoids at the 30% probability level, (b) macrocycle A, (c) the C–Br...H–C_{ester} contact involving ethyl acetate and (d) the inclusion process, with macrocycle B atoms depicted as van der Waals spheres.

In terms of molecular geometry differences, the two key *cisoid*-related Br1$_{A/B}$…Br3$_{A/B}$ distances are 4.4321(13) and 4.0315(11) Å in macrocycles A and B, respectively, whereas their pyridyl–N atoms are separated by 5.824(7) and 5.287(7) Å, with their C_5N planes mutually oriented at 56.9(3)° and 43.4(3)°, respectively. This geometric data suggests a measure of flexibility for these pyridyl groups that can be potentially exploited in future coordination chemistry. The range of the six key imide torsion angles (from torsion angle analysis as measured by their O=C…C=O angles, though labelled as **CO...CO**) spans *ca*. 23° (Table 2, SI).

In contrast, the isophthaloyl groups are considerably more flexible and adopt different conformations as noted by the much wider range of **OC...CO** torsions (Table 2, SI). The structural differences between macrocycles A and B can be accounted for by their local environments and the partial enclathration[20] that arises in both macrocycles. Overall, macrocycles A and B have similar conformations and are described as (*syn*)$_3$ or (**P**) based on the orientation of the three isophthaloyl *meta*-related carbonyl groups. This results in two parallel pyridinyl rings and this conformation dominates in **trezimide** chemistry.[13] The overlay of **Fmod**[2h] with the (**BrIO**)$_3$ **trezimide** shows a good fit for the scaffold non-hydrogen atoms (of 0.35 Å) and similar to the **tennimide** depicted in Scheme 4, though with some steric strain evident in (**BrIO**)$_3$ relative to the acyclic (2:1) imide **Fmod**.[2h]

The notable interactions in (**BrIO**)$_3$ involve halogen bonding with the bromine atoms Br3A (as Br…π_{arene}) and Br3B (as Br…O=C) (Table 2). The C–Br…π(arene) interaction with Br3A...C15/C16 distances of 3.424(6)/3.514(6) Å and the C34B–Br3B…O6B=C6B interaction (Br3B…O6B = 3.167(6) Å) assist in the (**BrIO**)$_3$ aggregation from 1–D zigzag chains into 2–D sheets. There are numerous but relatively weak, though cumulatively important, C–H…O=C/N hydrogen bonding interactions involving O1A, O5A (e.g. bifurcated hydrogen bonding linking H15A/H35A…O5A about inversion centres) and O3B. The ethyl acetate solvate forms a short contact as C14A–Br1A…H4S3–C4S (2.69 Å, 3.643(8) Å, 170°, 172°; N_c = 0.88) (Scheme 2, Table 2, Figure 1c),[11d-f,15] in tandem with a C33A–H33A…Br1A contact. The (**BrIO**)$_3$ crystal structure therefore, comprises a range of halogen and hydrogen bonding interactions aggregating from 1–D zigzag chains in tandem with inclusion and solvate effects.

(**BrIO**)$_4$ has a regular **tennimide** structure,[13] resides on a 2-fold crystallographic axis in space group *Pccn* (No. 56) and is relatively symmetrical (Figure 2a,b). The analogous methyl (**MIO**)$_4$ and chloro (**ClIO**)$_4$ **tennimides** also crystallise in the same space group and exhibit a measure of isostructurality.[21] In (**BrIO**)$_4$ the bromine sites are located as to approximate a tetrahedron with Br…Br distances from 11.0808(9) Å to 11.8026(15) Å and four intermediate distances of (11.1123(8) Å; 11.3021(8) Å). One of the pyridine rings (C21A, N22A,...,C26A) exhibits rotational disorder (50:50) necessitated by the close proximity of two symmetry–related *ortho*-H26A atoms on either side of the 2–fold axis (the bromine was modelled as one site with 100% site occupancy with only the pyridine C_5H_3N ring treated for (50:50) disorder during refinement, Figure 2a). A disordered chloroform molecule is located in a lattice void between the disordered pyridine rings on adjacent molecules and forms weak C–H...N interactions and Cl...O=C contacts [with N_c > 0.95] involving the $CHCl_3$, pyridine ring and carbonyl groups; the disorder precludes a thorough analysis.[15] The imide hinge (**CO...CO**) and isophthaloyl (**OC...CO**) torsion angle ranges in the scaffold are typical of **tennimides** (Figure 2b).[13] These highlight the regular and symmetrical nature of (**BrIO**)$_4$ as compared to the related (**26IO**)$_4$ **tennimide** that crystallises in three distinct conformational states as *cc* ↔ *oc* ↔ *oo* (*c/o = closed/open*).[13a] The present (**BrIO**)$_4$ structure is classed as having an *open-closed* conformation at the channel entrances and comparable in

geometric terms with the **(26IO)$_4$** *oc* conformation.[13a] There are no interactions of note involving the Br atoms apart from the Br14…C15 contact [Br…C 3.465(4) Å, C–Br…C 160.3(9)°, N_c = 0.98] about inversion centres and obviously hindered both by molecular and solvate disorder. This contrasts with the other four structures that all have significant halogen bonding interactions involving Br atoms (Table 2).

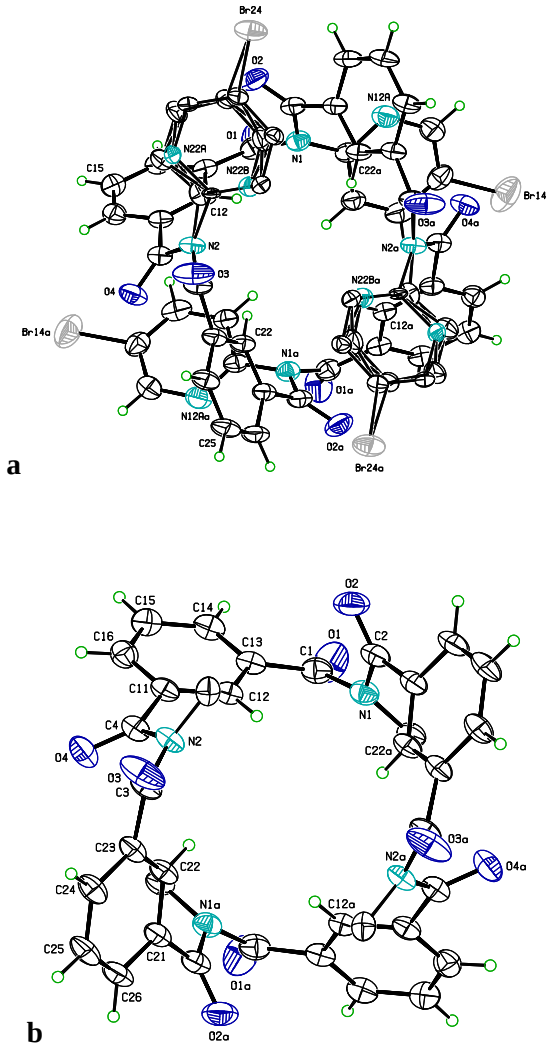

Figure 2. ORTEP diagrams of (*a*) **(BrIO)$_4$** with displacement ellipsoids at the 30% probability level; all pyridinyl H atoms are removed and (*b*) the **tennimide** core (with $CHCl_3$, pyridyl atoms removed for clarity, except for the *ipso*-$C_{pyridyl}$).

The **(26BrIO)$_3$ trezimide** was examined as two crystal structures with crystals grown from both $CHCl_3$ (Z'=2)[†] and CH_2Cl_2 (Z'=1)[‡]; the solvent molecules partially occupy macrocyclic niches and lattice voids. Both crystal structures (in triclinic space group $P\bar{1}$, No. 2) have **trezimide** structures with similar geometries that are distinctly asymmetric in shape as noted previously for **(BrIO)$_3$**. Both *a*, *b* unit cell lengths are similar but the *c* axis is almost twice as long in the $CHCl_3$ solvate[†], than for the CH_2Cl_2 solvate[‡]. Analysis reveals that the CH_2Cl_2 solvate structure is intermediate in structure between macrocycle A and B (of the $CHCl_3$ solvate).

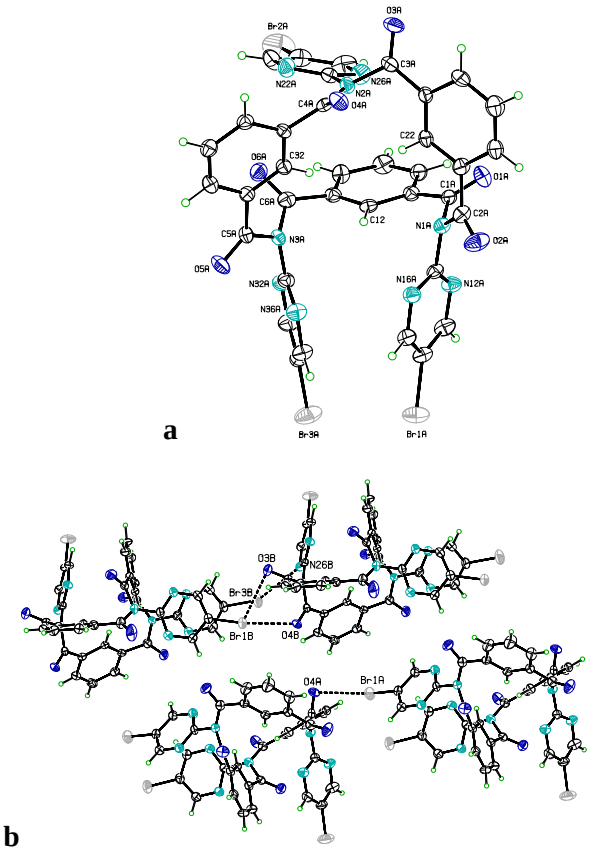

Figure 3. ORTEP views of **(26BrIO)$_3$**[†]as (a) macrocycle A with displacement ellipsoids at the 30% probability level and (b) macrocycles A and B highlighting the **C–Br**…**O=C**$_{carbonyl}$ 1–D directed halogen bonding (centre) ($CHCl_3$ solvate omitted for clarity).

In both **(26BrIO)$_3$** crystal structures (Figures 3,4), short C–Br...O=C intermolecular halogen bonding interactions[11,12] of 2.955(4) Å, 171.9(3)°; 3.036(4) Å, 150.9(2)° (ex–$CHCl_3$)[†] and 2.982(3) Å, 168.2(2)° (ex–CH_2Cl_2)[‡] are present (with $N_c \leq$ 0.90) directing aggregation as 1–D chains along the *b*– and *c*–axes, respectively, (Table 2). The two C–Br...O=C halogen bonds exhibit different geometries (in the $CHCl_3$ solvate[†]) with the longer (Br…O = 3.036(4) Å) classed as an interaction with the C=O$^{\delta-}$ π–cloud of C4A=O4A (Br…$C_{C=O}$ = 3.407(6) Å); several examples with similar dimensions are reported in the literature (Figure 3b).[15,22] The shorter interaction does not involve a Br…$C_{C=O}$ contact as Br4B…C4B = 3.605(5) Å. The Br...O interactions described above highlight the directional aspects of the C–Br...O halogen bonding and the relatively short Br...O intermolecular distances in the absence of strong electron–withdrawing groups (i.e. with aromatic rings containing one or more F atoms) that could further polarize the positive σ-holes on Br4A/B (Figures 3, 4).[11m-n] An estimate of the structural influence of substituting H with F (from $-C_6H_4Br$ to C_6F_4Br) would reduce the Br…O intermolecular distance by 0.1–0.2 Å (using structural data collated from molecules containing fluorinated bromobenzene rings).[15]

In the $CHCl_3$ structure,[†] amongst the plethora of weaker interactions and contacts, a distinct C24A–Br2A…π(arene) contact links chains of macrocycle A (about inversion centres) with Br2A…C34A/C35A = 3.366(6)/3.457(8) Å (N_c ≈ 0.95–0.97). This can be rationalised as the interaction of the positive σ-hole on Br2A with the aromatic π-cloud. Another interaction is noted involving a $CHCl_3$ solvent molecule (as Cl1-3C/C3S) which partakes in a short C–H…O [C3S…O1A = 3.004(11) Å] contact as well as two relatively short C–Cl…O contacts as Cl1C…O1A (3.127(6) Å, 151°) and Cl2C…O6A (3.004(6) Å, 161°): the latter directional as C–Cl…O (with N_c = 0.92), the former as Cl…O=C (N_c = 0.96) (SI).[15] Analysis of C–Cl…O contacts in >1000 structures on the CSD (with Cl…O < 3.27 Å, C–Cl…O 120–180°) reveals these as standard dimensions for contacts of this type. A second $CHCl_3$ solvate participates in C–H…$N_{pyrimidine}$ and C–Cl…O contacts.

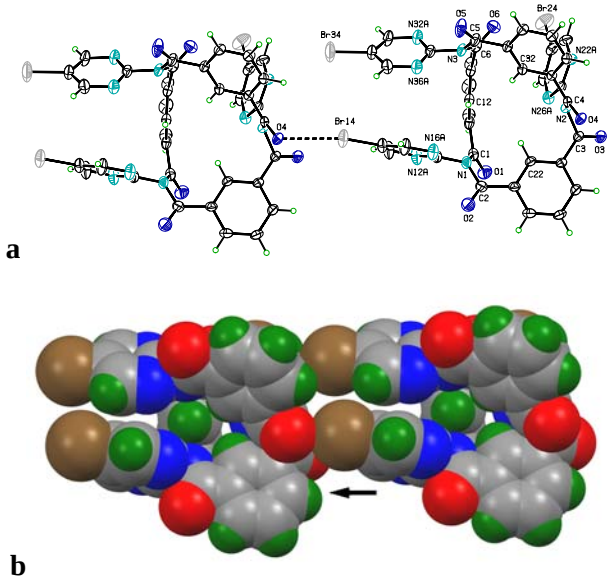

Figure 4. Views of (**26BrIO**)$_3$[‡] as (a) an ORTEP diagram with displacement ellipsoids at the 30% probability level and (b) a space filling model highlighting the primary **C–Br**...**O=C**$_{carbonyl}$ 1–D halogen bonding interaction.

In the (**26BrIO**)$_3$•CH_2Cl_2 solvate, the C14A–Br14...O4=C4 halogen bonding interaction (Figure 4) is augmented by C–H…O/Br contacts [as $R^3_3(6)$] linking 1–D chains parallel to the (110) plane. The C24–Br24...π(arene) contacts of 3.395(5), 3.362(5) Å (involving C34, C35, with angles of 162.8(2)°, 139.7(2)°, N_c ≈ 0.95–0.96) augments the primary 1–D halogen bonding into 2–D sheets, in addition to contacts involving both CH_2Cl_2 solvent molecules. All of these interactions highlight the unusual molecular aggregation in a crystal structure with molecules lacking strong classical hydrogen bond donors (that would typically form and dominate in preference to the halogen intermolecular interactions described above). However, in these structures the bromine atoms facilitate and direct 1–D chain formation as well as an exploration of more unusual interactions.

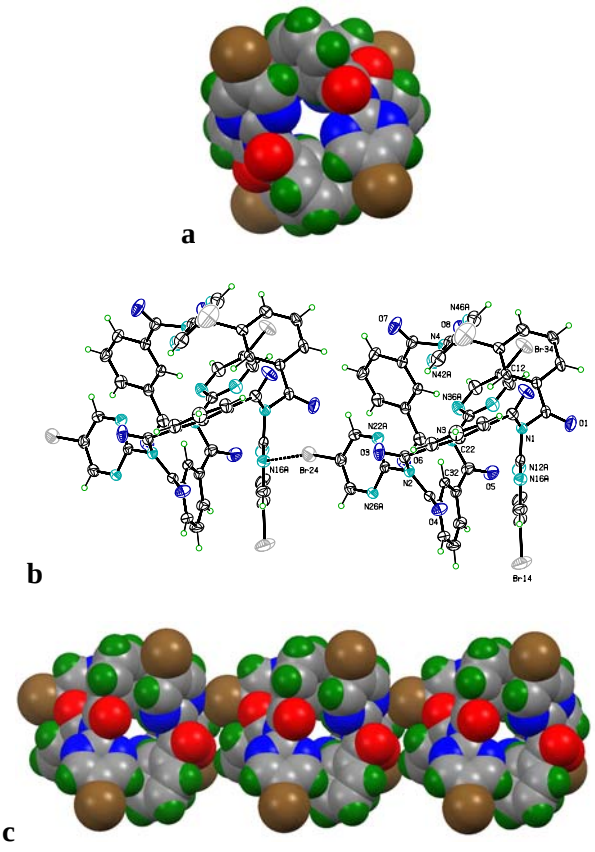

Figure 5. Views of (**26BrIO**)$_4$ as (a) a space filling model with the macrocyclic channel, (b) an ORTEP (with displacement ellipsoids at the 30% probability level) highlighting the **C–Br**...**N**$_{pyrimidyl}$ halogen bond and (c) a space filling model highlighting the 1–D chain of **C–Br**...**N** interactions and **tennimide** channel (solvent molecules omitted for clarity).

The (**26BrIO**)$_4$ molecular structure has a tetrahedral shape overall (Table 5, SI) and broadly similar to (**BrIO**)$_4$ but with distinct differences (Figure 5). These mainly derive from the influence of the sterically less-demanding pyrimidyl vs. pyridyl rings on the macrocyclic structure. The (**26BrIO**)$_4$ conformation is classed as *open–open* with respect to the molecular cavity as noted previously in one of the symmetrical parent **tennimides** (**26IO**)$_4$.[13a]

The C24A–Br24…N16A$_{pyrimidyl}$ halogen bond [3.028(4) Å, 165.5(2)°] with N_c = 0.89 links molecules into 1–D chains along the *b*-axis direction (Figure 5, Scheme 2) and augmented by weaker contacts involving the $CHCl_3$ molecules. The 1–D chains are linked into pairs aligned in opposite directions through an arrangement comprising the C15A–H15A…O4 and C14A–Br14…π(C24) contacts (as a combination of hydrogen and halogen bonded rings about inversion centres). There are also several C–H…O interactions involving the carbonyl O atoms (O3, O4, O5, O8) with O8 involved in a bifurcated H bonding arrangement weakly linking pairs of 1–D chains into a 2–D sheet and with the remaining O atoms weakly linking components into the 3–D structure. The N…Cl and C–H…Cl contacts involving the $CHCl_3$ solvate complete the intermolecular interactions.

In summary, the four brominated macrocycles enhance our knowledge of these relatively new classes of imide–based system.[9,13] In the **(BrIO)$_3$** and **(26BrIO)$_3$ trezimides**, the more common (**P**) or (*syn*)$_3$ conformation is observed with two heteroaromatic rings oriented in the same direction (with Br…Br separations of 4–5 Å). The **(BrIO)$_4$** and **(26BrIO)$_4$ tennimide** conformations are (*syn*)$_4$,[13] with the carbonyl torsion angle ranges reflecting the considerable twisting that arises due to greater flexibility within the isophthaloyl groups as compared to the imide hinges. The bromines form a variety of **C–Br**...**O=C**/**N**/π(arene) halogen bonds[11m,12] as well as weak hydrogen bonds. It is however, interesting to note that only 1 of the 3 or 4 bromines per macrocycle forms a short halogen bonding interaction and directs the formation of 1–D chains (the other Br atoms at most are involved in weaker interactions/contacts). We surmise that this is due to unfavourable orientations of the remaining Br atoms in forming additional halogen bonds. For these systems (without additional alkyl/aromatic F atoms to support in an auxillary manner) the influence of the Br σ-hole and the major role it plays in molecular aggregation is studied directly with an assessment of the role it plays in supramolecular assembly.

Conclusions

Brominated **trezimide** and **tennimide** imide–based macrocycles are synthesised in one step in modest yields,[13,21] with macrocycle formation relying on the non–planar imide *hinge* in macrocyclisation. **Trezimides** as (*syn*)$_3$ are asymmetric as influenced by the steric demands of the imide hinge, whereas **tennimides** adopt a symmetrical clasp–like scaffold with an internal molecular cavity large enough to accommodate a small atom/ion, though no enclathration has been observed thus far.[13] Analysis of the **C–Br**...**O=C**/**N** interactions facilitates an assessment of the structural role and effect of the positive σ-hole on the Br atoms,[11,12] its overall function in directing halogen bonding (especially in the pyrimidyls) and in driving 1–D chain formation. Future studies will focus on the development of coupling reactions using bromines[19] and metal coordination chemistry as well as their behaviour as potential transient storage systems for trapping and releasing molecules of interest (in larger imide-based macrocycles). The ability of halogen bonding to direct 1–D chain formation will be extended to studying larger 2–D/3–D assemblies.

Acknowledgements

This research is funded under the Programme for Research in Third Level Institutions (PRTLI) Cycle 4 (Ireland) and is co-funded through the European Regional Development Fund (ERDF), part of the European Union Structural Funds Programme (ESF) 2007–2013.

Notes and references

[a] School of Chemical Sciences, Dublin City University, Dublin 9, Ireland, Fax: +353-1-7005503, Tel: +353-1-7005114, E-mail: *john.gallagher@dcu.ie* Web: *http://doras.dcu.ie*

† Electronic Supplementary Information (ESI) available: Text, Tables, Figures and CIF files, providing NMR data (^{1}H-NMR including VT runs, COSY, NOESY, ^{13}C-NMR, DEPT, DEPTQ, HSQC, HMBC), infra-red (ATR), mass spectra, crystal structure data for five crystal structures as Tables 1–5 [(**26BrIO**)$_3$ as CH_2Cl_2[†] and $CHCl_3$[‡] solvates] for all new compounds. See DOI: 10.1039/b000000x/

1 W. Marckwald, *Chem. Ber.* 1894, **27**, 1317-1339.
2 a) A. E. Tschitschibabin, J. G. Bylinkin, *Chem. Ber.* 1922, **55**, 998, 1002; b) J. B. Wibaut, E. Dingemanse, *Recl. Trav. Chim. Pay-B.* 1923, **42**, 240-250; c) E. H. Huntress, H. C. Walter, *J. Org. Chem.* 1948, **13**, 735-737; d) P. A. Lyon, C. B. Reese, *J. Chem. Soc. Perkin Trans. 1*, 1974, **23**, 2645-2649; e) T. Suzuki, N. Kenbou, K. Mitsuhashi, *J. Heterocycl. Chem.* 1979, **16**, 645-648; f) L. W. Deady, D. C. Stillman, *Aust. J. Chem.* 1979, **32**, 381-386; g) K. Donnelly, J. F. Gallagher, A. J. Lough, *Acta Crystallogr., Sect. C: Cryst. Struct. Commun.,* 2008, **64**, o335-o340; h) J. F. Gallagher, K. Donnelly, A. J. Lough, *Acta Crystallogr., Sect. E: Struct. Rep. Online,* 2009, **65**, o102-o103; i) J. F. Gallagher, K. Donnelly, A. J. Lough, *Acta Crystallogr., Sect. E: Struct. Rep. Online,* 2009, **65**, o486-o487; j) J. F. Gallagher, S. Alley, A. J. Lough, *Acta Crystallogr., Sect. E: Struct. Rep. Online,* 2009, **65**, m332–m333.
3 E. E. Bolton, J. Chen, S. Kim, L. Han, S. He, W. Shi, V. Simonyan, Y. Sun, P. A. Thiessen, J. Wang, B. Yu, J. Zhang, S. H. Bryant, *J. Cheminf.* 2011, **3**, 32.
4 A. R. Murthy, S. D. Wyrick, P.J. Voorstad, I. H. Hall, *Eur. J. Med. Chem.* 1985, **20**, 547-550.
5 a) R. B. Seymour. G. S. Kirshenbaum, *High Performance Polymers: Their Origin and Development,* 1986, Elsevier, New York; b) D. Wilson, H. D. Stenzenberger, P. M. Hergenrother, *Polyimides*, 1990, Blackie & Son Ltd, Glasgow and London.
6 (a) J. Gawroński, M. Brzostowska, K. Gawrońska, J. Koput, U. Rychlewska, P Skowronek, B Nordén, *Chem. Eur. J.* 2002, **8**, 2484-2494; b) S. I. Kato, Y. Nonaka, T. Shimasaki, K. Goto, T. Shinmyozu, *J. Org. Chem.* 2008, **73**, 4063-4075; c) H. M. Colquhoun, Z. Zhu, D. J. Williams, C. J. Cardin, Y. Gan, A. G. Crawford, T. B. Marder, *Chem. Eur. J.* 2010, **16**, 907-918.
7 a) P. Osswald, D. Leusser, D. Stalke, F. Wurthner, *Angew. Chem. Int. Ed.* 2005, **44**, 250-253; b) F. Biedermann, E. Elmalem, I. Ghosh, W. N. Nau, O. A. Scherman, *Angew. Chem. Int. Ed.* 2012, **51**, 7739-7743.
8 a) S. V. Bhosale, C. H. Jani, S. J. Langford, *Chem. Soc. Rev*. 2008, **37**, 331-342; b) P. Ponnuswamy, F. B. L. Cougnon, J. M. Clough, G. D. Pantoş, J. K. M. Sanders, *Science* 2012, **338**, 783-785.
9 L. S. Evans, P. A. Gale, *Chem. Commun*. 2004, 1286–1287.
10 a) J. W. Steed, J. L. Atwood, J. L. *Supramolecular Chemistry*, **2009**, John Wiley & Sons, West Sussex, 2nd edn., 2009; b) J. W. Steed, P. A. Gale, *Supramolecular Chemistry: from Molecules to Nanomaterials,* Wiley, Hoboken, New Jersey, USA, 2012, *vol. 1-8.*
11 a) P. Metrangolo, G. Resnati, *Chem. Eur. J.* 2001, **7**, 2511-2519; b) A. de Santis, A. Forni, R. Liantonio, P. Metrangolo, T. Pilati, G. Resnati, *Chem. Eur. J.* 2003, **9**, 3974-3983; c) P. Auffinger, F. A.

Hays, E. Westhof, P. Shing Ho, *Proc. Nat. Acad. Sci. U.S.A* 2004, **101**, 16789-16794; d) P. G. Jones, P. Z. Kus, *Naturforsch*. 2007, **62**, 725-731; e) P. Metrangolo, F. Meyer, T. Pilati, G. Resnati, G. Terraneo, *Angew. Chem. Int. Ed*. 2008, **47**, 6114-6127; f) M. Mazik, A. C. Buthe, P. G. Jones, *Tetrahedron*, 2010, **66**, 385-389; g) Y. Lu, Y. Wang, W. Zhu, *Phys. Chem. Chem. Phys*. 2010, **12**, 4543-4551; h) R. D. Rogers, *Cryst. Growth Des*. 2011, **11**, 4721-4722; i) C. B. Aakeröy, P. D. Chopade, C. Ganser, J. Desper, *Chem. Commun*. 2012, 4688-4690; j) P. Metrangolo, G. Resnati, *Chem. Commun*. 2013, **49**, 1783-1785; k) H. R. Khavasi, A. A. Tehrani, *CrystEngComm*. 2013, **15**, 3222-3235; l) A. C. Legon, *Phys. Chem. Chem. Phys*. 2010, **12**, 7736-7747; m) R.W. Troff, T. Makela, F. Topic, A. Valkonen, K. Raatikainen, K. Rissanen, *Eur. J. Org. Chem*. 2013, **9**, 1617-1637; n) G. R. Desiraju, P. S. Ho, L. Kloo, A. C. Legon, R. Marquardt, P. Metrangolo, P. Politzer, G. Resnati, K. Rissanen, *Pure and Applied Chemistry*, 2013, **85**, 1711-1713.

12 a) K. E. Riley, J. S. Murray, P. Politzer, M. C. Concha, P. Hobza, *J. Chem. Theory Comput.* 2009**,** **5**, 155-163; b) Z. P. Shields, J. S. Murray, P. Politzer, *Int. J. Quantum Chem*. 2010, **110**, 2823-2832; c) M. Carter, P. Shing Ho, *Cryst. Growth Des*. 2011, **11**, 5087-5095; d) S. Tsuzuki, A. Wakisaka, T. Ono, T. Sonoda, *Chem. Eur. J*. 2012, **18**, 951-960; e) A. J. Parker, J. Stewart, J. K. Donald, C. A. Parish, *J. Am. Chem. Soc*. 2012, **134**, 5165-5172; f) P. Politzer, J. S. Murray, *ChemPhysChem*. 2013, **14**, 278-294.

13 a) P. Mocilac, J. F. Gallagher, *J. Org. Chem.* 2013, **78**, 2355-2361; b) P. Mocilac, J. F. Gallagher, *Acta Crystallogr. Sect. B: Struct. Sci.*, 2013, **69**, 62-69.

14 a) P. Mocilac, M. Tallon, A. J. Lough, J. F. Gallagher, *CrystEngComm* 2010, **12**, 3080-3090; b) P. Mocilac, A. J. Lough, J. F. Gallagher, *CrystEngComm* 2011, **13**, 1899-1909; c) P. Mocilac, J. F. Gallagher, *CrystEngComm* 2011, **13**, 5354-5366; d) P. Mocilac, K. Donnelly, J. F. Gallagher, *Acta Crystallogr., Sect. B: Struct. Sci.*, 2012, **68**, 189-203.

15 a) F. H. Allen, *Acta Crystallogr., Sect. B: Struct. Sci*., 2002, **58**, 380-388; b) F. H. Allen, W. D. S. Motherwell, *Acta Crystallogr., Sect. B: Struct. Sci.*, 2002, **58**, 407-422.

16 a) G. M. Sheldrick, *Acta Crystallogr., Sect. A, Found. Crystallogr.,* 2008, **64**, 112-122; b) P. McArdle, *J. Appl. Cryst*. 1995, **28**, 65.

17 a) C. F. Macrae, I. J. Bruno, J. A. Chisholm, P. R. Edgington, P. McCabe, E. Pidcock, L. Rodriguez-Monge, R. Taylor, J. van de Streek, P. A. Wood, *J. Appl. Cryst*. 2008, **41**, 466-470; b) A. L. Spek, *Acta Crystallogr., Sect. D, Biol. Crystallogr.,* 2009, **65**, 148-155.

18 G. P. Robertson, M. D. Guiver, M. Yoshikawa, S. Brownstein, *Polymer*, 2004, **45**, 1111-1117.

19 a) N. Miyaura, A. Suzuki, *Chem. Rev*. 1995, **95**, 2457-2483; b) I. P. Beletskaya, A. P. Cheprakov, *Coord. Chem. Rev*. 2004, **248**, 2337-2368.

20 a) J. F. Gallagher, G. Ferguson, V. Böhmer, D. Kraft, *Acta Crystallogr., Sect. C: Cryst. Struct. Commun.,* 1994, **50**, 73-77; b) J. Santamaría, T. Martín, G. S. Hilmersson, L. Craig, J. Rebek Jr., *Proc. Nat. Acad. Sci. U.S.A.* 1999, **96**, 8344-8347; c) D. Ajami, J.–L. Hou,; T. J. Dale, E. Barrett, J. Rebek Jr., *Proc. Nat. Acad. Sci. U.S.A.* 2009, **106**, 10430-10434.

21 P. Mocilac, Ph.D. Thesis, Dublin City University, 2012.

22 a) D. Damodharan, V. Pattabhi, M. Behera, S. Kotha, *J. Mol. Struct*. 2004, **705**, 101-106; b) S. Cruz, J. M. de la Torre, J. Cobo, J. N. Low, C. Glidewell, *Acta Crystallogr., Sect. E: Struct. Rep. Online*, 2006, **62**, o3056-o3058; c) H. Ziyat, M. Y. A. Ito, M. Ali,; A. Karim, A. Riahi, J.–C. Daran, *Acta Crystallogr., Cryst. Struct. Commun.*, 2006, **58**, o90-o93; d) M. Abboud, V. Mamane, E. Aubert, C. Lecomte, Y. Fort, *J. Org. Chem.* 2010, **75**, 3224-3231.

For Table of Contents Use Only

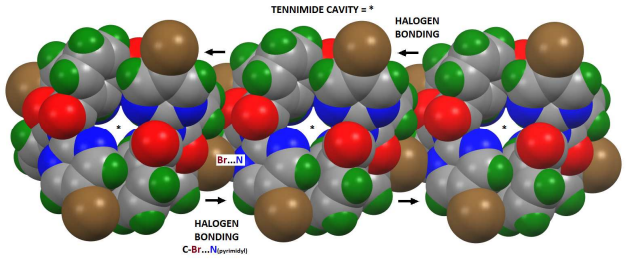

The imide–based **trezimide** and **tennimide** macrocycle crystal structures typically aggregate as 1–D chains through **C–Br**...**O=C**/**N**/π(arene) halogen bonds (with $N_c \leq 0.90$) that dominate the solid–state aggregation process in the absence of classical strong hydrogen bond donors.